Design of Inhibitors of Glycogen Phosphorylase: A Study of α- and β-*C*-Glucosides and 1-Thio-β-D-glucose Compounds†

Kimberly A. Watson,‡ Edward P. Mitchell,‡ Louise N. Johnson*,‡ Jong Chan Son,§ Claire J. F. Bichard,§ Michael G. Orchard,§ George W. J. Fleet,§ Nikos G. Oikonomakos,∥ D. D. Leonidas,∥ Maria Kontou,∥ and A. Papageorgiou∥

Oxford Centre for Molecular Sciences and Laboratory of Molecular Biophysics, The Rex Richards Building, South Parks Road, Oxford OX1 3QU, U.K., Dyson Perrins Laboratory, South Parks Road, Oxford OX1 3QY, U.K., and The National Hellenic Foundation, 48, Vas. Constantinou Avenue, Athens 11635, Greece

Received November 3, 1993; Revised Manuscript Received March 7, 1994®

ABSTRACT: α-D-Glucose is a weak inhibitor of glycogen phosphorylase *b* (K_i = 1.7 mM) and acts as a physiological regulator of hepatic glycogen metabolism. Glucose binds to phosphorylase at the catalytic site and results in a conformational change that stabilizes the inactive T state of the enzyme, promoting the action of protein phosphatase 1 and stimulating glycogen synthase. It has been suggested that, in the liver, glucose analogues with greater affinity for glycogen phosphorylase may result in a more effective regulatory agent. Several α- and β-anhydroglucoheptonic acid derivatives and 1-deoxy-1-thio-β-D-glucose analogues have been synthesized and tested in a series of crystallographic and kinetic binding studies with glycogen phosphorylase. The structural results of the bound enzyme–ligand complexes have been analyzed, together with the resulting affinities, in an effort to understand and exploit the molecular interactions that might give rise to a better inhibitor. This work has shown the following: (i) Similar affinities may be obtained through different sets of interactions. Specifically, in the case of the α- and β-glucose-*C*-amides, similar K_i's (0.37 and 0.44 mM, respectively) are obtained with the α-anomer through interactions from the ligand via water molecules to the protein and with the β-anomer through direct interaction from the ligand to the protein. Thus, hydrogen bonds through water can contribute binding energy similar to that of hydrogen bonds directly to the protein. (ii) Attempts to improve the inhibition by additional groups did not always lead to the expected result. The addition of nonpolar groups to the α-carboxamide resulted in a change in conformation of the pyranose ring from a chair to a skew boat and the consequent loss of favorable hydrogen bonds and increase in the K_i. (iii) The addition of polar groups to the α-carboxamide led to compounds with the chair conformation, and in the examples studied, it appears that hydration by a water molecule may provide sufficient stabilization to retain the chair conformation. (iv) The best inhibitor was *N*-methyl-β-glucose-*C*-carboxamide (K_i = 0.16 mM), which showed a 46-fold improvement in K_i from the parent β-D-glucose. The decrease in K_i may be accounted for by a single hydrogen bond from the amide nitrogen to a main-chain carbonyl oxygen, an increase in entropy through displacement of a water molecule, and favorable van der Waals contacts between the methyl substituent and nonpolar protein residues. (v) The β-hydrazide derivative showed an increase in K_i (0.4 mM) compared with β-*N*-methylamide, despite additional hydrogen bonds to the protein. Analysis of the binding interactions together with those of other compounds studied has shown the importance of desolvation effects. The energy required to dehydrate a compound on binding in the shielded environment of the catalytic site was not fully compensated by hydrogen bonds to the protein. (vi) Efforts to engineer additional hydrogen bonds did not always lead to a significant decrease in the K_i as might be predicted, partly as a result of the mixed polar/nonpolar nature of the binding pocket, of the necessity of dehydrating polar groups on transfer to the protein, and of the perturbation of the favorable binding mode of the glucosyl and amide portions of the molecules in order to make the additional hydrogen bond.

Knowledge of the three-dimensional structures of biological molecules has the potential to assist in the design of new therapeutic agents. From an analysis of the interactions between ligands and their macromolecules, insights into those interactions that most influence binding can be inferred and new ligands can be designed to exploit favorable interactions. There have been several encouraging examples where exploitation of biological structures has led to better inhibitors of enzymes and a deeper understanding of the molecular basis for drug target interactions. These studies may be viewed as the first stage toward new clinical compounds, studies that form part of an extended program in which other stages must address the much more difficult problems of drug delivery, drug targeting, toxicity, and side effects.

The pioneering work of Goodford and colleagues (Beddell et al., 1984) showed how the oxy/deoxy equilibrium of hemoglobin could be influenced by a bound ligand designed to produce a compound of relevance for the treatment of sickle cell anaemia. Other selected examples include several structurally different potent inhibitors of thymidylate synthase as potential anticancer agents (Appelt et al., 1991; Shoichet

† This work has been supported by the MRC (K.A.W. and E.P.M.), the Oxford Centre for Molecular Sciences (J.C.S., C.J.F.B., and M.G.O.), and an EEC Twinning Science programme (SC1*-CT91-0623) (N.G.O., D.D.L., M.K., and A.P.).

* Author to whom correspondence should be addressed.

‡ Oxford Centre for Molecular Sciences and Laboratory of Molecular Biophysics.

§ Dyson Perrins Laboratory.

∥ The National Hellenic Foundation.

® Abstract published in *Advance ACS Abstracts,* April 15, 1994.

0006-2960/94/0433-5745$04.50/0

et al., 1993), inhibitors of the salvage pathway of the enzyme purine nucleoside phosphorylase (Ealick et al., 1991), inhibitors of carbonic anhydrase for the control of fluid balance in the eye (Baldwin et al., 1992), C_2-symmetric phosphinate inhibitors of human immunodeficiency virus protease (Abel-Meguid et al., 1993), and potent sialidase-based inhibitors of influenza virus replication (van Itzstein et al., 1993), or a fuller understanding of the molecular basis of existing drugs, such as antiviral agents against the common cold virus (Chapman et al., 1991; Kim et al., 1993) or against the human immunodeficiency virus reverse transcriptase (Kohlstaedt et al., 1992; Jacobo-Molina et al., 1993).

In this study, we approach a systematic examination of glucose analogue inhibitors of glycogen phosphorylase (GP[1]) that eventually may be of clinical interest in the regulation of glycogen metabolism in diabetes. The studies have shown that binding modes can be unpredictable, but may be rationalized with the benefit of structural data, and that a buried catalytic site poses problems for the systematic addition of binding groups.

Glycogen is the carbohydrate reserve of most metabolically active cells in mammals. Cellular demands to produce glucose 1-phosphate (Glc-1-P) from glycogen are met by the large regulatory enzyme GP, which catalyzes the degradative phosphorylation of glycogen to glucose 1-phosphate (Glc-1-P). In muscle, Glc-1-P is utilized via glycolysis to provide energy to sustain muscle contraction, and in the liver it is converted to glucose to provide fuel for other tissues. The activation and inhibition of phosphorylase are under hormonal, neuronal, and metabolic control. The enzyme may be viewed as a regulator, selecting between positive effectors that promote glycogen degradation (such as adrenaline or calcium signals that result in activation by phosphorylation and metabolites P_i, glycogen, and AMP) and negative effectors that inhibit degradation and allow the cell to store glycogen for later use (such as insulin-induced signals for dephosphorylation, glucose, ATP, and glucose 6-phosphate). The positive allosteric effectors promote a catalytically active R state, while the negative effectors inhibit by stabilizing the inactive T state (Johnson et al., 1989; Newgard et al., 1989; Johnson, 1992).

In response to nervous or hormonal signals, the enzyme is converted from the *b* form (predominantly T state) to the *a* form (predominantly R state) through the phosphorylase kinase catalyzed addition of a phosphate to the hydroxyl group of Ser14, located near the N-terminus of the molecule. The reverse reaction of dephosphorylation that inactivates the enzyme is catalyzed by protein phosphatase 1 (PP1), an enzyme that is regulated in response to insulin (Dent et al., 1990) and that promotes glycogen synthesis through its activation of glycogen synthase. PP1 is the major enzyme that activates glycogen synthesis and also the principal enzyme that inactivates the enzymes of glycogenolysis (GP and phosphorylase kinase). In muscle, PP1 is regulated in response to insulin and adrenaline by phosphorylation of a glycogen binding subunit [reviewed by Cohen (1992)]. In the liver, the glycogen binding subunit does not appear to be controlled by phosphorylation/dephosphorylation events, and instead the dephosphorylation of glycogen synthase by hepatic PP1 is inhibited allosterically by low concentrations of phosphorylase *a*. This inhibition is mediated by the glycogen binding subunit (Alemany & Cohen, 1986; Bollen & Stalmans, 1992).

[1] Abbreviations: GP, glycogen phosphorylase; Glc-1-P, α-D-glucose 1-phosphate; PP1, protein phosphatase 1; GP*a* and GP*b*, glycogen phosphorylase *a* and *b* forms, respectively; NIDDM, non-insulin-dependent diabetes mellitus; BES, *N*,*N*-bis(2-hydroxyethyl)-2-aminoethanesulfonic acid.

The effects of GP on the glycogen binding subunit appear to be distinct from the recognition of GP as a substrate by the catalytic subunit of PP1. Glucose is a physiological regulator of hepatic glycogen metabolism that promotes the inactivation of GP (Stalmans et al., 1974; Hers, 1976) and acts synergistically with insulin (Witters & Avruch, 1978; Hartman et al., 1987). Glucose inactivates GP*a* by competitive inhibition with the substrate Glc-1-P and by favoring the T-state conformation. The T-state conformation is a better substrate for the protein phosphatase than the R state (Madsen et al., 1978, 1983; Sprang et al., 1982), and formation of GP*b* relieves the inhibition of PP1 and promotes the activation of glycogen synthase. Thus, the balance between glycogen degradation and glycogen synthesis is controlled by phosphorylation and dephosphorylation events, and these events are modulated by other metabolites, notably glucose.

The aim of this study was to design better regulators of GP that could shift the balance from glycogen degradation to glycogen synthesis. Such compounds eventually may be of therapeutic interest. Hyperglycemia in non-insulin-dependent diabetes mellitus (NIDDM) is a result of diminished insulin release and/or insulin resistance, which leads to impaired tissue glucose uptake and impaired suppression of hepatic glucose production (DeFronzo, 1988). At basal insulin levels, impaired suppression of the hepatic output of glucose is the principal cause of high glucose concentrations in NIDDM patients. In response to insulin release after eating, muscle glycogen synthesis is the major method of glucose disposal. In the diabetic patient, insulin does not exert its normal effects (to lower blood glucose levels) and fails to stimulate the synthesis of glycogen.

Several glucose analogues have been synthesized and used in a three-dimensional crystallographic binding study of GP. The three-dimensional structures of T-state rabbit muscle GP*b* (Acharya et al., 1991) and the glucose–GP*b* complex (Martin et al., 1990) have been used as models for the design of glucose analogues (Martin et al., 1991). It is known that glucose itself is a weak, competitive inhibitor of GP (K_i = 1.7 mM) and in a self-regulatory system helps to lower blood glucose levels by the inhibition of glycogen degradation through direct action on GP and the promotion of glycogen synthesis by modulating the PP1/GP recognition properties as described above. It has been postulated that, in the liver, glucose analogues with greater inhibition of GP may result in more effective regulatory agents than glucose. Although the three-dimensional structure of liver phosphorylase is not known, the amino acid sequence has 80% overall identity to the rabbit muscle sequence and has 100% identity between residues involved in the catalytic site (Newgard et al., 1986).

We report crystallographic and kinetic investigations of a number of α- and β-glucoheptonamides and β-thioglucose analogue inhibitors of T-state rabbit muscle GP based on guidelines previously established. Through an analysis of the phosphorylase–glucose analogue complex structures, we identify the dominant molecular interactions that determine the different affinities and show how these have led to improved inhibition constants.

EXPERIMENTAL PROCEDURES

Materials. The syntheses of compounds **1–28** are reported elsewhere (J. C. Son, C. J. F. Bichard, and G. W. J. Fleet, manuscript in preparation). 1-Thio-β-D-glucose (sodium salt), AMP, glucose 1-phosphate, and glycogen were purchased from Sigma.

Kinetic Studies. The kinetic studies were performed as described previously (Martin et al., 1991). Phosphorylase

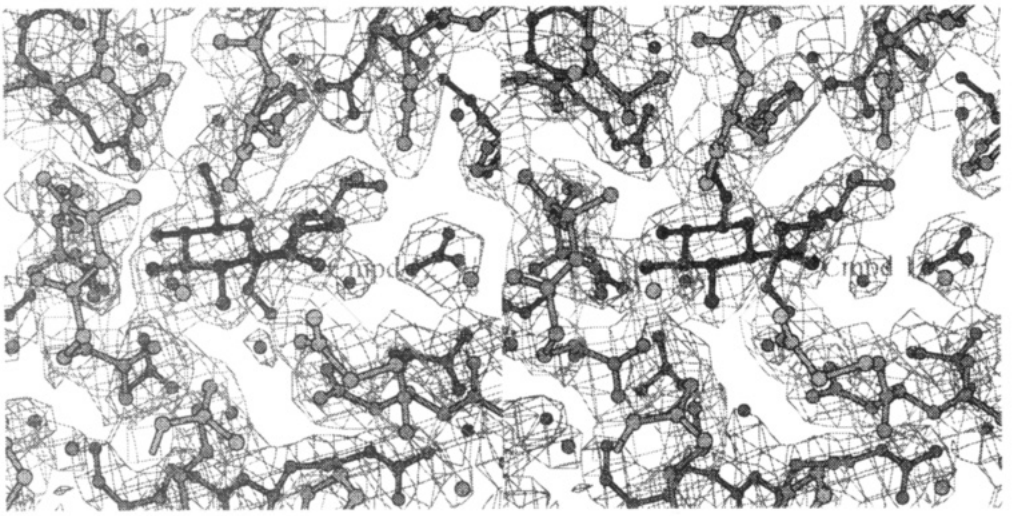

FIGURE 1: Stereo diagram of a final $2F_o - F_c$ electron density map in the region of the glucose analogue **12** bound at the catalytic site of GP*b*. The contour level corresponds to 3 rms deviations of the map. This figure and others was produced interactively using the program XOBJECTS (M. E. M. Noble, unpublished work).

was assayed in the direction of glycogen synthesis at pH 6.8 and 30 °C by measuring the release of inorganic phosphate. The enzyme (5–20 μg/mL) was assayed in 47 mM triethanolamine hydrochloride (pH 6.8), 100 mM KCl, 1 mM DTT, 1 mM EDTA, 1% glycogen, and 1 mM AMP with concentrations of Glc-1-P between 3 and 20 mM and concentrations of glucose analogues as indicated in the Results. Initial velocities were calculated from pseudo-first-order reaction constants (Engers et al., 1970). Enzyme preparations exhibited V_{max} values of 70–80 μmol mg^{-1} min^{-1} (with respect to Glc-1-P) and K_m values for Glc-1-P of 1.2–2.2 mM at saturating AMP (1 mM) and glycogen (1%). Kinetic data were analyzed by Michaelis–Menten kinetics using nonlinear regression analysis (Leatherbarrow, 1987). Hill coefficients were generated by linear regression analysis of Hill plots. K_i values were determined by plotting K_m(app) versus inhibitor concentration, with an explicit value for the standard deviation of each point.

Crystallographic Binding Studies. Crystals of T-state GP*b* were grown as detailed previously (Oikonomakos et al., 1985; Johnson et al., 1974). Prior to data collection, T-state GP*b* crystals were soaked for 1 h in a buffered solution [10 mM *N,N*-bis(2-hydroxyethyl)-2-aminoethanesulfonic acid (BES) and 0.1 mM ethylenediaminetetraacetic acid (EDTA) (pH 6.7)] containing approximately a 100 mM concentration of the compound of interest. One crystal was used for each experiment. In each case, 2.3-Å resolution data were collected on a Nicolet IPC multiwire area detector using a Rigaku RU-200 rotating anode X-ray source with a graphite monochromator, operating between 50 kV/50 mA and 60 kV/60 mA. The detector was placed 16 cm away from the crystal and at a swing angle of 22°. Data frames of 0.2° oscillation were collected with exposure times ranging between 90 and 120 s. The data frames were processed with either the XENGEN (Howard et al., 1987) or XDS (Kabsch, 1988a,b) package of programs to produce a scaled set of structure factors, which was then used to generate difference Fourier electron density maps (with respect to the native protein) using the SERC (UK) Collaborative Computing Project No. 4 (CCP4) suite of programs for protein crystallography (Daresbury, UK).

Refinement of the enzyme complexes was performed on a Convex C210 using X-PLOR energy and crystallographic least-squares minimization (Brunger, 1988, 1989; Brunger et al., 1989). Individual atomic *B*-factor refinement was performed in the final cycles of the refinement. The starting protein structure was the refined structure of the glucose complex (Martin et al., 1990). The starting structure for each of the ligands was generated using ideal bond lengths, bond angles, and torsion angles with the program Sybyl (Tripos Assoc., 1992). The glucosyl moiety was maintained in the standard conformation as observed in the glucose–GP complex. Additional groups were added in their standard minimum energy conformation, and if necessary, adjustments were made to torsion angles to fit the groups to the observed difference density. Water molecules in the glucose–GP*b* complex were examined, and those displaced by the ligand were removed. Simulated annealing was not performed during the refinements, since the difference maps did not indicate substantial changes from the glucose–GP*b* complex. Final difference Fourier ($2F_o - F_c$) electron density maps were calculated using the X-PLOR refined coordinates for each of the ligand–phosphorylase complexes. A portion of a final electron density map in the region of the catalytic site is shown (Figure 1) for compound **12** bound to GP*b*. Estimates of the precision of coordinates taken from previous studies indicate errors on the order of 0.2 Å in positional coordinates.

A display of density maps and refined structures was performed using the molecular graphics program Frodo (Jones, 1978, 1985) implemented on an Evans and Sutherland PS390 graphics terminal. Potential hydrogen bonds were assigned if the distance between two electronegative atoms was less than 3.3 Å and if the angle formed between these two atoms and the preceding atom was greater than 90°. van der Waals interactions were assigned where the separation between nonhydrogen atoms was less than 4 Å.

RESULTS

Comparison of the crystal structures of the less active T state and the more active R state of GP (Barford & Johnson, 1989; Barford et al., 1991) has shown two essential changes at the catalytic site of GP that characterize the allosteric transition. Firstly, in the T state access to the catalytic site is blocked by a loop of chain from residues 282 to 286 (termed the 280s loop), and in the R state this loop is displaced. Secondly, displacement of the 280s loop removes an acidic residue from the catalytic site (Asp283), and this side chain is replaced by the side chain of a basic residue (Arg569) to create a high-affinity phosphate recognition site. Both the movement of the arginine and the movement of the 280s loop

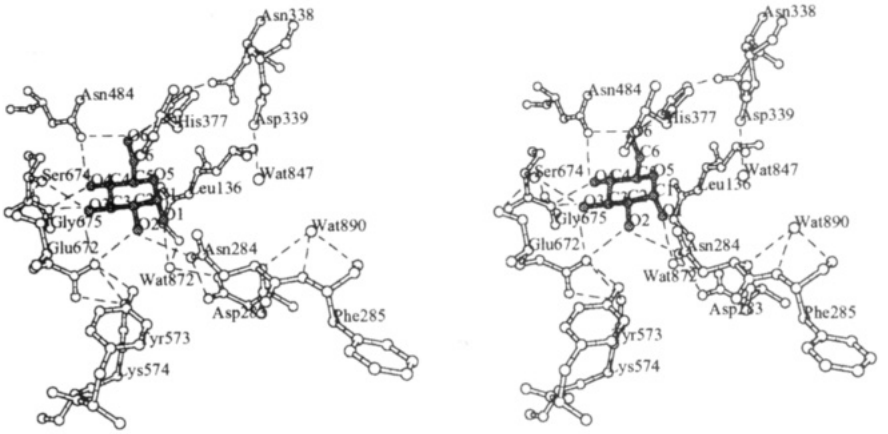

FIGURE 2: Binding of α-D-glucose to the catalytic site of GP*b* (K_i = 1.7 mM). Stabilization of the T state is through hydrogen bonds from O1 via OH8 Wat872 to Asp283 and from O2 directly to Asn284.

Table 1: Glucose Analogue Inhibitors and Their Kinetic Constants for Glycogen Phosphorylase *b*[a]

compound	substituents at C1-position α	substituents at C1-position β	concentrations used (mM)	K_i (mM)	*n*
1	C(=O)NH_2	H	1, 2, 3	0.37 ± 0.03	1.5
2	C(=O)NHCH	H	40	36.7 ± 5.6	1.4
3	C(=O)$NHCH_2CH_2OH$	H	20, 40	16.9 ± 4.4	1.4
4	C(=O)NHC_6H_5-4-OH	H	20	12.6 ± 2.0	1.3
5	C(=O)NH-4-OHC_6H_4	H	20, 30	5.6 ± 0.5	1.1
6	C(=O)$NHCH_2$-2,4-$F_2C_6H_3$	H	10	27.2 ± 5.2	1.0
7	C(=O)$NHNH_2$	H	5	3.0 ± 0.7	1.3
8	C(=O)NHNH-2,4-$(NO_2)_2C_6H_3$	H	1, 1.5, 2	0.7 ± 0.1	1.3
9	COOH	H	5, 10	1.62 ± 0.02	1.7
10	$COOCH_3$	H	40	24.2 ± 6.4	1.5
11	H	C(=O)NH_2	0.5, 1, 1.5, 2	0.44 ± 0.07	1.3
12	H	C(=O)$NHCH_3$	0.3, 0.5, 1	0.16 ± 0.03	1.2
13	H	C(=O)$NHCH_2CH_2OH$	5, 10	2.6 ± 0.2	1.1
14	H	C(=O)NHC_6H_5	15	5.4 ± 0.4	1.4
15	H	C(=O)NH-4-OHC_6H_4	10	4.4 ± 0.7	1.6
16	H	C(=O)$NHCH_2$-2,4-$F_2C_6H_3$	10	8.6 ± 1.2	1.0
17	H	C(=O)$NHNH_2$	2, 3	0.4 ± 0.1	1.1
18	H	C(=O)$NHNHCH_3$	5, 10	1.8 ± 0.3	1.7
19	H	C(=O)$NHCH_2CF_3$	10	8.1 ± 1.8	1.0
20	H	C(=O)NHCHCH$_2$CH$_2$	10	1.3 ± 0.3	1.5
21	H	COOH	5, 10	NI	
22	H	$COOCH_3$	10, 15	2.8 ± 0.1	1.7
23	H	SH	2, 3, 5	1.0 ± 0.1	1.5
24	H	$SCH_2C(=O)OCH_2CH_3$	5, 10, 20	NI	
25	H	$SCH_2C(=O)NH_2$	20	21.1 ± 6.8	1.0
26	H	$SCH_2C(=O)NHC_6H_5$	10	3.6 ± 0.4	1.1
27	H	$SCH_2C(=O)$NH-2,4-$F_2C_6H_3$	10	18.9 ± 3.1	1.0
28	H	$SCH_2C(=O)$NHNH-2,4-$(NO_2)_2C_6H_3$	2, 4	0.65 ± 0.01	1.2

[a] NI, not inhibitory.

are correlated with changes at the subunit interface, and through these concerted movements substrate binding at the catalytic site can be communicated to the phosphorylation site, which is over 30 Å away, and *vice versa*.

Glucose binds at the catalytic site of GP buried 15 Å from the surface and close to the essential cofactor, pyridoxal phosphate. The binding is dominated by hydrogen bonds from each of the peripheral hydroxyl groups to protein atoms, such that each hydroxyl is involved both as a donor and as an acceptor of hydrogen bonds (Martin et al., 1990, 1991). In particular, the α-1-OH is hydrogen-bonded through water (OH8 Wat872) to Asp283, and the 2-OH group is hydrogen-bonded directly to Asn284 (Figure 2). These interactions help keep the 280s loop in its localized position characteristic of the T state and provide an explanation for the ability of glucose to promote the T state, in addition to acting as a competitive inhibitor with the glucosyl moiety of Glc-1-P. Only one water (OH9 Wat904) located near the 2-OH hydroxyl is displaced by the glucose moiety. There are 56 van der Waals contacts between glucose and the enzyme. However, there is only moderate complementarity of van der Waals contacts between nonpolar ligand and protein groups, and there are no aromatic/glucopyranose interactions. These observations, together with the involvement of fewer charged groups in hydrogen-bond interactions, provide an explanation (Martin et al., 1991) for the 10^4-fold lower affinity of GP for glucose than, for example, in the high-affinity periplasmic monosaccharide binding proteins (Quiocho, 1989). The enzyme–glucosyl recognition site has an empty pocket for substituents in the β-configuration at C1. Further, at the α-C1-position there is a water-filled channel leading to the 280s loop. The sites at the α- and β-positions of C1 have been the target for additional groups to provide a tighter inhibitor than glucose itself.

The compounds studied and their associated kinetic data (K_i) and Hill coefficients are summarized in Table 1. The crystallographic results of 21 glucose analogue–GP complexes studied are shown in Table 2. Some of the potential inhibitors were not studied in detail. The α-acid **9** cracked the crystals. Adjustment of concentration in the range from 100 to 10 mM

Table 2: Crystallographic Data Collection and Refinement Statistics

compound	no. of reflections measured	no. of unique reflections[a]	$\langle I/\sigma \rangle$ or *no. of reflections $I/\sigma > 12$	$R_m(I)$[b]	R_{iso}[c]	no. of reflections used in refinement[d]	final R[e]
1	85 299	34 496	10.8	0.092	0.132	34 397	0.206
2	75 943	33 834	13.9	0.075	0.119	31 675	0.182
3	80 933	36 123	13.9	0.101	0.148	32 580	0.207
4	81 489	32 920	14.2	0.081	0.139	32 384	0.205
5	81 516	34 858	15.8	0.075	0.129	34 580	0.204
6	84 967	34 878	13.0	0.073	0.111	34 845	0.210
7	66 142	28 690	23218*	0.052	0.086	27 807	0.171
10	83 643	35 345	15.5	0.074	0.100	35 182	0.198
11	105 513	37 191	15.2	0.071	0.117	37 038	0.199
12	75 782	31 386	18843*	0.070	0.115	30 474	0.173
13	82 436	33 185	13.6	0.071	0.119	33 120	0.197
14	76 382	30 367	26450*	0.056	0.106	29 511	0.174
15	76 247	31 917	23790*	0.048	0.108	30 976	0.172
16	75 923	29 225	27858*	0.051	0.133	28 372	0.179
18	87 975	27 056	23585*	0.064	0.130	26 082	0.165
19	87 014	31 042	18725*	0.095	0.118	29 952	0.175
20	86 796	33 884	26951*	0.101	0.126	32 862	0.184
22	75 631	31 953	24582*	0.055	0.099	31 028	0.174
25	80 363	33 940	16.1	0.067	0.093	33 801	0.198
26	76 149	30 499	28158*	0.076	0.113	29 593	0.175
27	73 845	30 646	19881*	0.104	0.096	29 753	0.178

[a] Data sets were between 72% and 92% complete to 2.3-Å resolution. [b] Merging R factor: $R_m = \sum_i \sum_h (|I(h) - I_i(h)|)/I_i(h)$, where $I(h)$ and $I_i(h)$ are the mean and ith measurement of intensity for reflection h. [c] Mean fractional isomorphous difference in structure factor amplitudes from native T-state GP*b*. [d] Reflections between 8- and 2.3-Å resolution. [e] Crystallographic R factor: $\sum||F_o| - |F_c||/\sum|F_o|$, where $|F_o|$ and $|F_c|$ are the observed and calculated structure factor amplitudes, respectively.

and careful checks on pH led to no improvement; consequently, there were no structural data for this compound. Compounds **21** and **24**, which were found to be noninhibitory from the kinetic analysis, were not studied in the crystal. Both dinitrophenyl compounds (**8** and **28**) were found to bind at the inhibitor site in addition to the catalytic site. The difference Fourier maps arising from these complexes were analyzed, but the structures were not refined.

In a previous study (Martin et al., 1991) of glucose analogue inhibitors bound to GP, the best inhibitor was α-(hydroxymethyl)-1-deoxyglucose, whose K_i (1.5 mM) was similar to that of α-D-glucose (K_i = 1.7 mM). The hydroxymethyl group in the α-(hydroxymethyl)-1-deoxyglucose–GP complex made a direct hydrogen bond to the main-chain nitrogen of Leu136, while in the glucose–GP complex, the α-OH group of α-D-glucose is hydrogen-bonded through water to Asp283. The similarity in K_i's of these two compounds suggests that the two different hydrogen bonds (one through water and the other directly to the protein) in the different complexes have approximately equal strengths. The work suggested that it should be possible to exploit both hydrogen-bonding capacities in the design of a better inhibitor. A number of α- and β-glucoheptonic acid derivatives (compounds **1–22**, Table 1) were synthesized and studied in kinetic and crystallographic experiments.

α-Glucoheptonic Acid Derivatives. The α-heptonamide **1** has a K_i = 0.37 mM and binds almost 5 times more tightly than glucose. The crystallographic analysis showed that the glucosyl moiety of α-heptonamide **1** made hydrogen bonds to the protein similar to those glucose (Table 3). At 2.3-Å resolution, the difference between oxygen and nitrogen atoms in the electron density cannot be distinguished. Hence, there is an ambiguity in the orientation of the amide group. Two possible conformations that differed by 180° in the torsion angle about C1–C7 were explored in the refinement. Both gave similar crystallographic R values and similar temperature factors for the relevant atoms. However, in one conformation the NH_2 group of the amide came within 2.9 Å of the ND2 atom of Asn284, and this unfavorable contact led us to choose the alternative conformation. In this orientation, the torsion angle O5–C1–C7–N is −88°, the carbonyl oxygen is hydrogen-bonded to OH0 Wat887, and the amide NH_2 group is hydrogen-bonded to OH8 Wat872 (Figure 3 and Table 4a). [OH8 Wat872 is hydrogen-bonded to N Gly135 and OD1 Asp283, and OH0 Wat887 is hydrogen-bonded to N Leu136, N Gly134, and OE2 Glu88.] There is an additional contact from the amide carbonyl oxygen to N Leu136 that is slightly too long (3.5 Å) for a hydrogen bond. The two hydrogen bonds formed confirmed the expectation for the bifunctional group, although the hydrogen bond through water to N Leu136 was not predicted.

Table 3: Summary of the Polar Contacts between the Glucose Analogue Ring Hydroxyls of Select Inhibitors and the Catalytic Site Residues of GP*b*[a]

		compound and distance (Å)				
glucose atom	protein atom	α-D-glucose	**1**	**2**	**11**	**12**
O2	OH8 Wat872	–	–	2.9	–	–
	ND2 Asn284	3.2	3.3	–	3.1	3.1
	OE1 Glu672	2.9	3.2	–	2.9	3.0
	OH7 Wat890	3.0	3.2	–	3.1	3.1
	OH Tyr573	–	–	–	3.2	3.1
O3	OH7 Wat890	–	–	3.2	–	–
	OE1 Glu672	2.9	2.9	2.9	2.8	2.9
	N Ala673	–	–	2.8	–	–
	N Ser674	3.0	3.1	3.2	3.1	3.2
	N Gly675	3.0	3.2	–	3.0	3.0
O4	OD1 Asn484	3.1	–	–	–	3.3
	N Gly675	2.8	3.0	2.6	2.8	2.9
	OH1 Wat897	2.6	2.5	2.6	2.6	2.6
O6	ND1 His377	2.7	2.9	2.7	2.7	2.7
	OD1 Asn484	3.0	2.9	3.2	2.8	3.0

[a] Polar contacts between α-D-glucose and GP*b* are given for comparison. –: indicates contact is greater than 3.3 Å.

Following crystallographic analysis of the α-heptonamide **1**, modeling of other compounds was performed. The glucosyl moiety in its bound $^4C_1$ chair conformation at the catalytic site was fixed and substituents were added. Torsion angles were adjusted to allow favorable interactions with the protein. This led to a series of compounds (**2–10**) in which the $^4C_1$ chair geometry of the glucosyl part and the O5–C1–C7–N torsion angle allowed additional substituents on the amide nitrogen to extend in the direction of the β-pocket of the active site. Using these models as a guide, several compounds were

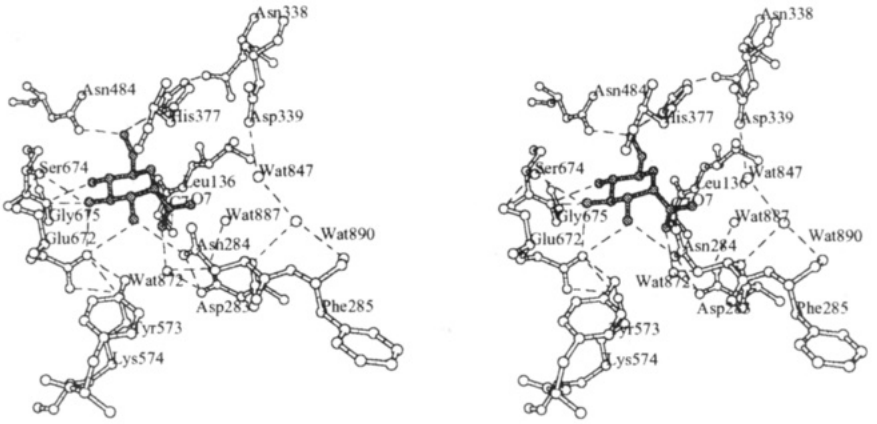

FIGURE 3: Contacts between the α-glucoheptonamide **1** (K_i = 0.37 mM) and GP*b* show potential hydrogen bonds between the carbonyl oxygen O7 and OH0 Wat887 and between the amide nitrogen N and OH8 Wat872.

synthesized with the aim of exploiting residues in the β-pocket while maintaining favorable contacts from the amide portion of the inhibitor to residues in the α-pocket.

However, modification of the α-heptonamide **1** by the addition of an *N*-methyl group led to a surprising result, since it was predicted that the addition of the methyl group would displace the water (OH0 Wat887) and lead to improved inhibition. In fact, the methyl amide **2** was a much poorer inhibitor than the amide, with a K_i of 36.7 mM. The crystallographic analysis gave a difference electron density map in which the glucose analogue was well-defined and in which the substituent at the C1-position appeared to be equatorial with respect to the glucopyranose ring and not axial as expected for a compound with the α configuration. The single-crystal structure of compound **2** showed that the glucosyl moiety did not have the standard $^4C_1$ chair conformation, but had a skew boat conformation, which places substituents at the α-C1 in equatorial geometry (Watson et al., 1993). The skew boat conformation was found to fit the electron density for the methylheptonamide–phosphorylase complex, and the structure refined well.

The torsion angles for the glucopyranose ring are compared with those for glucose in Table 5. The change in structure from chair to skew boat allows some hydrogen bonds from the glucosyl component to the enzyme, but the contacts to the O2 hydroxyl that are made in the glucose complex are lost in the complex with the methyl amide **2** (Table 3 and Figure 4). There are no hydrogen bonds to the amide group. These differences provide an explanation for the lower affinity of the methylheptonamide **2** compared with the α-heptonamide **1** (Table 1). The skew boat conformation is observed both in the single-crystal structure and in the phosphorylase complex and, hence, does not appear to be a result of either lattice packing effects or binding to phosphorylase.

Compounds **3**–**6** were also found, from binding studies to phosphorylase, to have skew boat geometry (Table 5), but compounds **7**, **8**, and **10** bound with $^4C_1$ chair geometry. The reasons for the different ring geometries for the different α-heptonamides are not clear. Carbohydrate conformation is influenced by stereoelectronic effects; for example, the anomeric effect (Lemieux & Koto, 1974) usually results in electronegative α-substituents of glucose analogues being placed in an axial orientation. Steric and solvent effects, as shown with *C*-glycosides, may also be important (Goekjian et al., 1991). It seems that compounds with small, polar substituents (e.g., **1** and **7**) may adopt a chair conformation, but those with more bulky nonpolar groups (**2**–**6**) adopt a skew boat conformation. The C1-substituents of dinitrophenyl hydrazide **8** (chair conformation) are bulky and have both polar and nonpolar character, but the polar groups are proximal to the C-amide. The importance of solvent effects may be illustrated by the observations that the chair conformation with the α-C1-substituents axial could be stabilized by hydration when the additional groups are polar, but such stabilization is not possible for nonpolar groups.

Examination of the structures when bound to phosphorylase shows that there is a protein-bound water molecule that can hydrogen bond to polar substituents, but which would repel, or be displaced by, nonpolar groups (Figure 5). In **1** the amide nitrogen hydrogen bonds to water OH8 Wat872 (Figure 3), while in **7** the carbonyl oxygen and the second nitrogen hydrogen bond to this water (Figure 5a). In the methyl ester **10**, one of the oxygens is hydrogen-bonded to the water and the methyl group is directed away from the water by a suitable rotation about the oxygen–carbon bond (Figure 5b). In the methyl amide **2**, the amide partial double bond does not allow such a rotation, and as a result the methyl group would be placed too close to the water if compound **2** adopted the same ring conformation as compounds **1** or **7**.

It seems that solvation effects may be important in favoring the chair conformation for polar substituents, and these effects could operate for both the enzyme-bound compounds and those in solution. Such a hypothesis would need to be substantiated by a larger body of experimental data and single-crystal structures of the relevant compounds. We have previously reported the single-crystal structure of methyl amide **2** (Watson et al., 1993). Attempts to crystallize some of the other α-glucoheptonamides were not successful. It is concluded that both the chair and skew boat conformations are accessible to the amido derivatives of D-*glycero*-D-*ido*-heptonic acid, but that the conformation is influenced in a subtle way by the nature of the substituent groups and solvation effects

The structural results provided an explanation for the poor affinity of **2** compared with **1**. The kinetic results show that hydroxyethyl amide **3** has an improved K_i compared with **2** (K_i(**3**) =16.9 mM versus K_i(**2**) = 36.7 mM). In the final $2F_o - F_c$ electron density map, the hydroxyethyl group has weak density compared with the glucopyranosyl ring, but the position of the hydroxyl group as located in the refinement allows a hydrogen bond to OD1 Asp339 (distance, 2.8 Å) (Table 4a). This additional hydrogen bond could account for the improved binding energy difference of 0.5 kcal/mol. The anilide **4** shows a K_i of 12.6 mM. In the complex with **4**, and in contrast to the complex with **3**, the contact between O7 and N Leu136 is close enough for a hydrogen bond (Table 4a). In addition, some binding energy may be obtained from van der Waals interactions with the phenyl group. There are 15 van der Waals interactions between the phenyl group and the protein,

Table 4: Interactions between GP*b* and the C1-Substituent Atoms of the Glucose Analogues

(a) Polar Contacts between GP*b* and C1-Substituent Atoms[a]

compound	atom numbering	ligand atom	protein atom	distance (Å)
α-D-glucose	O1	O1	OH8 Wat872	3.0
1	C7(=O7)N	O7	OH0 Wat887	3.3
		N	OH8 Wat872	2.8
3	C7(=O7)NC8C9O8	O8	OD1 Asp339	2.8
4	C7(=O7)N-phenyl	O7	N Leu136	3.3
5	C7(=O7)N-*p*-phenol-O11	O11	NE2 His341	2.7
6	C7(=O7)NC8-*o*,*p*-difluorophenyl	O7	N Leu136	3.2
7	C7(=O7)N1N2	O7	OH8 Wat872	2.8
		N2	OHO Wat887	2.7
			OD1 Asp283	2.6
			OH8 Wat872	2.7
10	C7(=O7)O7C8	O7	OH8 Wat872	2.9
			N Leu136	3.3
11	C7(=O7)N	O7	ND2 Asn284	2.8
		N	O His377	2.9
12	C7(=O7)NC8	N	O His377	3.1
15	C7(=O7)N-*p*-phenol-O11	O11	NE2 His341	2.9
			OH2 Wat890	3.1
17	C7(=O)N1N2	N1	O His377	2.9
		N2	OH4 Wat847	3.0
18	C7(=O7)N1N2C8	N1	O His377	3.0
19	C7(=O7)NC8C9F_3	N	O His377	2.8
20	C7(=O7)CHCH$_2$CH$_2$	O7	ND2 Asn284	3.0
		N	O His377	3.3
26	SC7C8(=O8)NPh	O8	OH0 Wat877	3.2
		N	OD1 Asp339	3.3
27	SC7C8(=O8)N-*o*,*p*-difluorophenyl	O7	N Asn284	2.9
		N	OD1 Asp339	2.9

(b) Summary of the Polar Contacts and the van der Waals Interactions

compound	no. of hydrogen bonds	no. of van der Waals contacts	waters displaced by C1-substituents
1	2	13	none
2	none	11	none
3	1	17	OH4 Wat847
			OH2 Wat890
4	1	23	OH4 Wat847
			OH2 Wat890
5	1	18	OH4 Wat847
			OH2 Wat890
6	1	53	OH4 Wat847
7	4	20	none
10	2	14	none
11	2	11	none
12	1	14	OH4 Wat847
13	none	16	OH4 Wat847
14	none	28	OH4 Wat847
15	2	37	OH4 Wat847
16	none	43	OH4 Wat847
			OH2 Wat890
17	2	17	OH2 Wat890
18	1	22	OH4 Wat847
19	1	32	OH4 Wat847
20	2	18	OH4 Wat847
			OH2 Wat890
22	none	15	OH4 Wat847
			OH2 Wat890
23	1	4	none
25	3	31	OH4 Wat847
			OH2 Wat890
26	1	40	OH4 Wat847
			OH2 Wat890
27	2	51	OH4 Wat847
			OH2 Wat890

[a] Potential hydrogen bonds are assigned if the distance between two electronegative atoms is less than 3.3 Å and if the angles formed between these two atoms and the preceding atom is greater than 90°.

the most important of which are to the side chains of Leu136, His341, and Thr378 (Table 4b). An explanation for the similarity in the K_i values of **3** and **4** is that the energy difference (approximately 0.5–0.6 kcal/mol) between removal of the hydroxyethyl group from water and the resulting hydrogen bond of the hydroxyl to Asp339 (as observed for the complex with **3**) is roughly equivalent to the removal of the phenyl group from water and its resulting van der Waals contacts and a hydrogen bond to O7 (as observed in the complex with **4**).

The hydroxy anilide **5** gives a further reduction in K_i (K_i(**5**) = 5.6 mM). There is a hydrogen bond between the hydroxyl

Table 5: Torsion Angles for the Glucopyranose Ring Atoms of Compounds **2**–**6**[a]

atoms	compound	torsion angle (deg)
C1–C2–C3–C4	α-D-glucose	−51.3(1)
	2	26.9(3)
	3	13
	4	20
	5	12
	6	14
C2–C3–C4–C5	α-D-glucose	53.3(1)
	2	31.1(3)
	3	44
	4	39
	5	45
	6	42
C3–C4–C5–O5	α-D-glucose	−57.5(1)
	2	−64.8(3)
	3	−74
	4	−71
	5	−69
	6	−69
C4–C5–O5–C1	α-D-glucose	62.2(2)
	2	33.7(3)
	3	37
	4	37
	5	31
	6	30
C5–O5–C1–C2	α-D-glucose	−60.9(2)
	2	27.0(3)
	3	23
	4	24
	5	29
	6	27
O5–C1–C2–C3	α-D-glucose	54.1(2)
	2	−59.7(3)
	−50	**3**
	4	−54
	5	−51
	6	−53

[a] Torsion angles for both α-D-glucose and compound **2** are those obtained from the small molecule X-ray crystallographic analyses. Torsion angles for compounds **3**–**6** are those obtained from the X-PLOR refined enzyme–ligand complexes.

group and NE2 of His341, but the contact from O7 to N Leu136 is long for a hydrogen bond (3.7 Å). Comparison of the K_i's for **4** and **5** suggests an energy difference of about 0.4 kcal/mol. Thus, both **3** and **5** make a hydrogen bond from their additional hydroxyl group to the enzyme, but it appears that in order to make these interactions a potential hydrogen bond between the O7 atom and N Leu136 is lost. Compound **4**, which lacks a hydroxyl group, is able to make this latter hydrogen bond. The longer side chain in the difluorobenzyl amide **6** results in a poor inhibitor (K_i = 27.2 mM). The electron density for the difluorobenzyl group is weak, and the refinement resulted in high temperature factors for the side-chain group and the glucosyl moiety. The difluorobenzyl group is placed farther into the β-pocket. There is room for this group, but there are few favorable van der Waals interactions and no favorable interactions with the fluorine atoms. The carboxyl group of Asp339 is stacked almost normal to the phenyl group, an arrangement that appears unfavorable for a potential charged/aromatic interaction, but which could allow some favorable interaction (Burley & Petsko, 1986) if the aspartate were protonated, as seems likely (Martin et al., 1991). As for the anilide **4**, in the absence of definite favorable interactions of the side-chain groups with the protein, the O7 is hydrogen-bonded to N Leu136 (Table 4a).

The hydrazide **7** is of interest because, in contrast to the methyl amide **2**, it bound in the chair conformation and, in contrast to the primary amide **1**, the assignment of the orientation of the amide group was defined by the additional electron density for the second nitrogen. The torsion angle for O5–C1–C7–N1 was 88° (compared with −88° for **1**) and that for C1–C7–N1–N2 was −170°. As a result of the different torsion angle, the amide group of **7** does not make the favorable hydrogen bonds observed for **1**, but the N2 group is hydrogen-bonded directly to OD1 Asp283 and both the N2 and O7 atoms are hydrogen-bonded through water OH8 Wat872 to Asp283. The van der Waals contacts from N of the amide to ND2 Asn284 and to N Leu 136 are satisfactory. Despite the contacts to Asp283, which might be anticipated to favor the T state of the enzyme, the Hill coefficient (n = 1.3, Table 1) for **7** indicates that it is not as effective as glucose. The K_i values of **1** and **7** (0.37 and 3.0 mM, respectively) do not appear compatible with the interactions observed. Compound **7** fails to make the hydrogen bonds to the amide that are observed in the compound **1** complex, and some compensation for this loss from the hydrogen bonds from the N2 atom in the compound **7** complex should result in more similar K_i values. The explanation for the 10-fold difference in K_i may reside in the energy required to dehydrate **7** on transfer to the binding site in the enzyme. This is discussed further in the comparison of compounds **12** and **17**.

The dinitrophenyl hydrazide **8** showed a further variation in the O5–C1–C7–N1 torsion angle (= 172°). The difference electron density showed clear binding of this compound with all atoms, including the two nitro groups well-resolved. The dinitrophenyl group is sandwiched between the side chains of Asn284 and Tyr573, and the bulky group causes conformational changes. His571 is displaced and the whole of the main chain in the 280s loop (residues 282–286) shifts. However, the position of the side chain of Phe285 is barely altered. The nucleoside inhibitor site of the phosphorylase molecule is occupied by a second molecule of **8**, in which only the dinitrophenyl moiety is localized. An explanation for the reduced K_i of **8** compared with other compounds in this series may be provided by the occupation of the inhibitor site, which provides additional binding energy. Because of the multiple binding modes, it is not possible to distinguish individual contributions. The Hill constant of 1.3 (Table 1) for **8** indicates that it is a poorer T-state inhibitor than glucose, which has a Hill coefficient of 1.5.

The α-carboxylic acid **9** (K_i = 1.6 mM) showed an increase in K_i compared to the methyl amide **2** (K_i = 0.37 mM) and a dramatic increase in the Hill coefficient (n = 1.7), but the compound cracked the crystals and no structural data are available. The crystallographic analysis showed that α-methyl ester **10** (K_i = 24 mM) bound with the glucopyranose ring in chair geometry. The torsion angle O5–C1–C7–O8 is 81°, similar to that observed for the hydrazide **7**. The O7 oxygen hydrogen bonds to N Leu136 and water OH8 Wat872, which is hydrogen-bonded to an additional water, Asp283, and N Gly135 (Table 4a). The position of O7 is similar to the carbonyl oxygen of the primary amide in **1**. However, the O8 oxygen, in contrast to the NH_2 group in **1**, makes no hydrogen bonds. The O8 oxygen and the methyl group are 3.3 Å from CB Leu136 and 3.0 Å from ND2 Asn284, respectively, and these polar/nonpolar contacts may account for the poor inhibition. In addition, the glucosyl moiety is shifted slightly, so that the hydrogen bonds to O2 are reduced to one, compared with three observed in glucose. The polar contacts that appear to favor a chair conformation have been discussed previously.

β-Glucoheptonic Acid Derivatives. The β-series of glucoheptonic acid derivatives were synthesized to complement the α-series. The β-configuration allows the substituent atoms to follow the β-pocket more naturally than in the α-series, and modeling studies showed that Asp339 and His341 could be

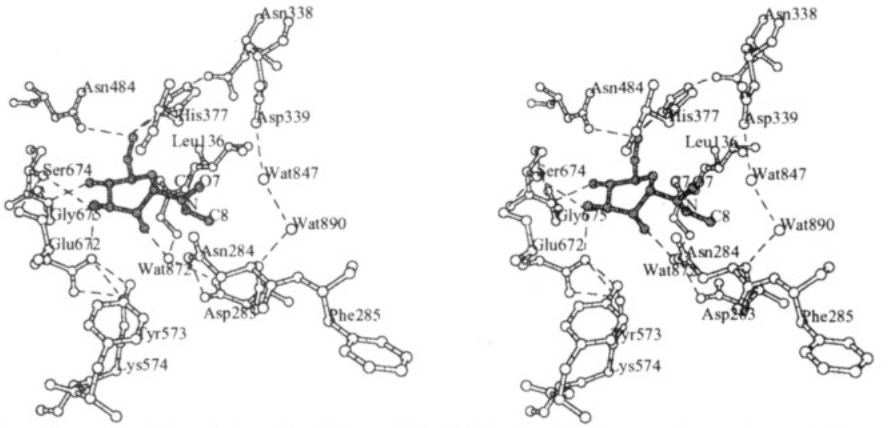

FIGURE 4: Binding of the α-heptonic acid methyl amide **2** (K_i = 36.7 mM) in the skew boat conformation to GP*b*. In this conformation, close contact of the nonpolar methyl substituent with OH8 Wat872 is avoided. Loss of potential hydrogen bonds to O2 and lack of hydrogen bonding to the amide moiety provides an explanation for the increase in K_i.

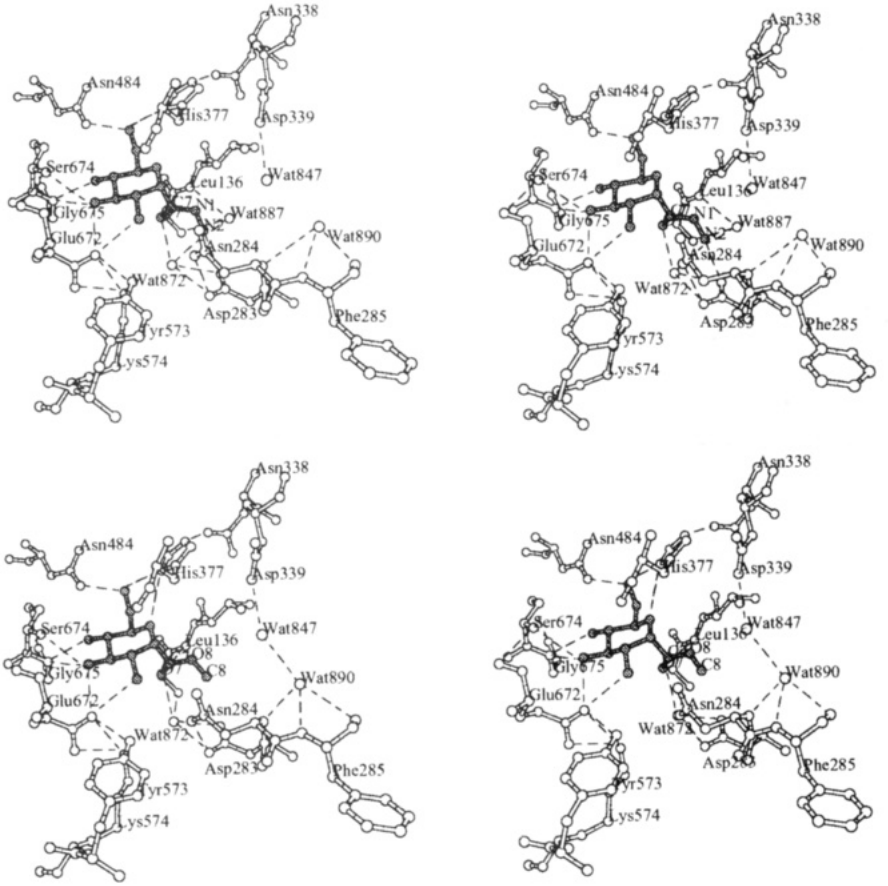

FIGURE 5: Comparison of the binding of α-heptonic acid hydrazide **7** with α-methyl ester **10**. (a, top) Contacts between the α-heptonic acid hydrazide **7** (K_i = 3.0 mM) and GP*b* show potential hydrogen bonds from the polar groups on C1 (carbonyl oxygen O7 and the hydrazide nitrogen N2) to OH8 Wat872. (b, bottom) Contacts between the α-methyl ester **10** (K_i = 24.2 mM) and GP*b* show only one potential hydrogen bond between the carbonyl oxygen O7 and OH8 Wat872. Freedom of rotation around the C7–O8 bond allows the close contact of the methyl substituent and OH8 Wat872 to be avoided with the chair conformation of the ring.

targeted by large polar groups and Asn284 and His377 by smaller groups.

The β-series showed a more consistent pattern of interactions without the complication of the chair/skew boat transformations. In the complex with the β-amide **11**, the amide group makes two hydrogen bonds directly to protein atoms. The NH_2 group hydrogen bonds to O His377 and the carbonyl oxygen O7 bonds to ND2 Asn284, but the latter hydrogen bond is bent by about 50° from the plane of the donor amide of Asn284 (Figure 6a, Table 4a). The α- and β-amides **1** and **11** have similar K_i values (0.37 and 0.44 mM, respectively). The structural analysis shows that these similar K_i values are achieved with different interactions in the two complexes (Table 4a).

The β-methyl amide **12** is the best inhibitor in the heptonamide series, with a K_i of 0.16 mM. There is only one hydrogen bond from the amide nitrogen to O His377, and the O7 atom is just too far away from ND2 Asn 284 to make a hydrogen bond (Table 4a, Figure 6b). The methyl group makes six van der Waals contacts, of which three are to nonpolar groups in residues His377 and Thr378 and three are to polar groups in residues Asp339 (OD1), His377 (O), and Asn284 (ND2) (Table 4b). A water molecule, OH4 Wat847, which would be 2.8 Å from the methyl group, is displaced, and it appears that the increase in entropy from the release of this water, together with the van der Waals interactions to the methyl group, may account for the 3-fold decrease in K_i of **12** compared to **11** (0.6 kcal/mol). In the complex with

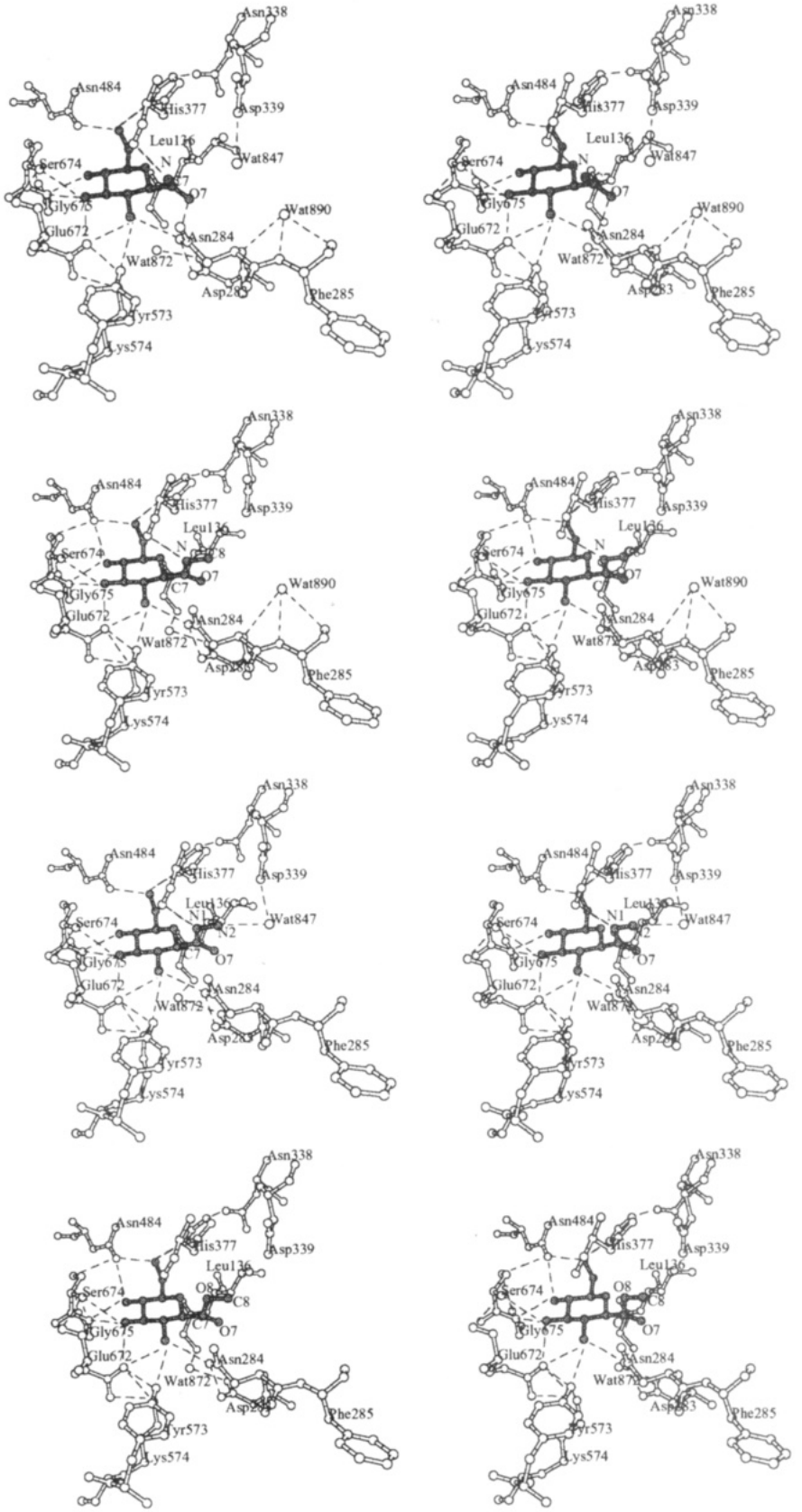

FIGURE 6: Comparison of the binding of β-glucoheptonamide **11**, β-heptonic acid methyl amide **12**, β-heptonic acid hydrazide **17**, and β-methyl ester **22**. (a, top) Contacts between the β-glucoheptonamide **11** (K_i = 0.44 mM) and GP*b* show two potential hydrogen bonds from the amide moiety directly to protein atoms (O7 to ND2 Asn284 and N to O His377). A similar K_i to compound **1** is achieved through different interactions with the enzyme. (b, second) Binding of the β-heptonic acid methyl amide **12** (K_i = 0.16 mM) to GP*b* gives rise to the best inhibitor in the heptonamide series. The decrease in K_i may be accounted for by a single hydrogen bond from the amide nitrogen N directly to the protein O His377, by an increase in entropy through the displacement of OH4 Wat847, and by van der Waals contacts between the methyl C8 and nonpolar groups in residues His377 and Thr378. (c, third) The β-heptonic acid hydrazide **17** (K_i = 0.4 mM) binds in a similar mode to compound **12** (b). OH4 Wat847 is not displaced and forms a hydrogen bond to the polar hydrazide nitrogen N2. OH2 Wat890 is only weakly bound and is partially displaced. Other similarities in hydrogen bonds and van der Waals contacts suggest that differences in the K_i's arise as a result of increased energy required to dehydrate the hydrazide upon transfer to the buried catalytic site of GP*b*. (d, bottom) The β-methyl ester **22** (K_i = 2.8 mM) binds in a mode similar to **12** (b) and **17** (c). Additional loss of hydrogen bonds from the C1-substituents to the protein leads to a further increase in the K_i.

the hydroxyethyl amide **13**, OH4 Wat847 is displaced, and the hydroxyl group is placed at the position of the displaced water and is hydrogen-bonded to Asp339. The explanation for the increase in the K_i of **13** (2.6 mM) compared to **12** (0.16 mM) may be that in order to make the hydrogen bond with the hydroxyl group, the amide is slightly displaced so that the distance from N to O His377 is now too long for a strong hydrogen bond. Further, the ethyl group is displaced relative to the methyl group of **12**, so that the C8 and C9 atoms of **13** make no favorable van der Waals contacts and C9 is 2.9 Å from OD1 Asp339, a slightly unfavorable distance for a van der Waals contact (Table 4b). Modeling suggests that the hydroxymethyl amide might have been a better group, but this compound is unlikely to be chemically stable.

Complexes with the anilides **14** and **15** show almost identical orientations for the phenyl group. The aromatic group fits in the pocket with 23 van der Waals interactions to the ring, of which 11 are to nonpolar groups from residues Leu136 and Thr378 (Table 4b). However, the hydrogen bonds to the amide are less favorable than those in **11**. The distances of O7 to ND2 Asn284 and N to O His377 are 3.3 Å, compared with 2.8 and 2.9 Å in **11**. In both complexes with **14** and **15**, the plane of the carboxyl group of Asp339 has flipped 90° about the CB–CG bond with respect to its position in the complexes with **11** and **12**. The carboxyl group is normal to the aromatic ring. The closest approach is from C10 to OD1 Asp339 (3.3 Å), and this contact could represent a weak aromatic/polar hydrogen bond. However, the oxygen atom of the carboxyl group is 20–30° from the plane of the aromatic ring, whereas in other structures where more definite hydrogen-bridging interactions are observed the acceptor oxygen is in the plane of the aromatic ring (Burley & Petsko, 1988). There are small shifts of the glucosyl group, so that the hydrogen bonds to this group are perturbed. It is concluded that the poorer K_i values of **14** and **15** are a consequence of the small adjustments in the protein structure and the glucosyl moiety needed to accommodate the phenyl ring, which lead to slightly poorer interactions that are not compensated by van der Waals interactions. The hydroxyl group in **15** is hydrogen-bonded to NE2 His341 and OH2 Wat890, but these hydrogen bonds appear to make little contribution to the binding energy (the K_i of **15** is 4.4 mM, whereas the K_i of **14** is 5.4 mM). A possible rationalization is given in the Discussion. The difluorobenzyl amide **16** bound poorly, with indications of movement of protein atoms. Its binding was not analyzed in detail.

The hydrazide **17** bound in a mode very similar to the methyl amide **12** (Figure 6c). However, the water OH4 Wat847 is not displaced and the N2 atom is hydrogen-bonded to this water, which in turn is hydrogen-bonded to Asp339. A second water OH2 Wat890 appears to be weakly bound and is partially displaced. The N1 nitrogen is hydrogen-bonded to O His377 (2.9 Å, Table 4a). The amide oxygen O7 to ND2 Asn284 contact is 3.3 Å and is bent (45° from the plane), so that here, as in **12**, there is no hydrogen bond. Compound **17** is a slightly poorer inhibitor than compound **12** (the K_i of **17** is 0.4 mM and the K_i of **12** is 0.16 mM). The van der Waals interactions of the methyl in **12** or the N2 in **17** appear comparable. In the complex with **12**, there are six van der Waals interactions, three with polar groups and three with nonpolar groups; in the complex with **17**, there are seven van der Waals interactions, three with polar and four with nonpolar groups (excluding hydrogen bonds). A possible explanation for the difference in K_i may lie in the energy required to dehydrate the hydrazide functionality of **17** in order to transfer it to the buried environment of the protein. The energy of dehydration may not be compensated by the hydrogen bond to the water at the binding site. With the methyl amide **12**, there is less compensatory energy required for dehydration and probably some gain from shielding the nonpolar group from bulk water. In addition, the water OH4 Wat847 is displaced in the methyl amide complex, leading to an increase in entropy. The need to compensate for dehydration may explain why, in a number of compounds where an additional hydrogen bond was engineered (e.g., **1** and **7**, **12** and **17**, and **14** and **15**), there is not a dramatic improvement in K_i, as might be expected from the energy of a hydrogen bond.

The methyl hydrazide **18** is a poorer inhibitor than the unsubstituted hydrazide **17**. The hydrazide group is characterized by torsion angles O5–C1–C7–N1–N2–C8 of 91°, 180°, and 143°, respectively. The additional methyl group displaces the water OH4 Wat847, and there is no hydrogen bond from the second nitrogen, N2. The N2 is just too far from Asn284 to make a hydrogen bond to OD1 (3.7 Å), and the planar amide bond does not allow any adjustment to shorten the contact. The C8 methyl group is placed 3.3 and 3.2 Å from OD1 and OD2, respectively, of Asp339, and although these contacts are within the limits for van der Waals interactions, this is not a favorable environment for a methyl group. The trifluoroethyl amide **19** is a worse inhibitor than the methylhydrazide **18**, and predictably this is because the fluorine atoms are placed close to Asp339 (closest contact, 2.9 Å). The cyclopropyl amide **20** presents a rigid nonpolar group, and the atoms occupy space similar but not identical to those observed for the complex with the trifluoroethyl derivative **19**. The cyclopropyl amide **20** is a better inhibitor than **19** (K_i(**20**) = 1.8 mM; K_i(**19**) = 8.1 mM) and comparable to the methyl hydrazide **18** (K_i = 1.8 mM). Compound **20** makes not only some satisfactory van der Waals contacts to the nonpolar groups of Leu136 and Thr378 but also some van der Waals contacts (>3.8 Å) to the carboxyl side chain of Asp339. The carboxyl side chain of Asp339 has flipped 90° to a position similar to that observed in complexes with **14**, **15**, and **18**, and this observation indicates that the flip is not necessarily associated with a hydrogen-bridging interaction with an aromatic group.

In order to accommodate the cyclopropane group in the pocket, there has been some shift of the glucosyl and amide moieties with respect to their positions in the methyl amide **12**. The bent hydrogen bond from the carbonyl oxygen O7 to ND2 Asn284 is 3.0 Å, and the hydrogen bond from the NH of the amide to O His377 is just 3.3 Å (Table 4a). Three of the hydrogen bonds to the glucose moiety are just outside the 3.3-Å cutoff. Kinetic studies showed that β-carboxylic acid **21** was not inhibitory, and this compound was not studied crystallographically.

The β-methyl ester **22** is bound in a manner almost identical to that of the β-methyl amide **12**. The methyl groups occupy similar positions, but the ester group in contrast to the amide group makes no hydrogen bonds (Figure 6d). The O7 oxygen is 3.5 Å from ND2 Asn284. The O8 oxygen is 3.5 Å from O His377 and it cannot participate as a donor, in contrast to **12** where the NH group makes a hydrogen bond. The water OH4 Wat847 is displaced in complexes with both **12** and **22**. These similarities in binding modes suggest that the major explanation for the 18-fold difference in K_i values (K_i(**12**) = 0.16 mM; K_i(**22**) = 2.8 mM) comes from the hydrogen bond that is made to O His377 in the complex with **12**. Calculations indicate that this hydrogen bond contributes about 1.7 kcal/mol to the binding energy.

Thioglucose Analogues. β-D-Glucose has a poor K_i (7.6 mM; Martin et al., 1991). The mixed polar/nonpolar

character of the β-pocket led us to consider replacing the polar β-OH group of β-D-glucose with a nonpolar group that could be easily polarized. Accordingly, the β-1-thio compounds were explored. 1-Thio-β-D-glucose **23** was found to exhibit an improved K_i (1.0 mM) compared with β-D-glucose. In the crystal complex, the thio group makes van der Waals contacts to ND2 Asn284 (3.4 Å), O His377, CB His377, and OH4 Wat847. The structure of the thiolate ion suggests that there could be an interaction between the S^- and Asn284. However, in the crystallographic experiments, the pH of the solution was carefully adjusted to pH 6.7, and at this pH the thiol is expected to be the dominant form. The substituted thio compounds **24–28** are all poorer inhibitors than the β-thioglucose **23**. The ethyl ester **24**, which was noninhibitory, was not studied crystallographically. The acetamide **25** showed weak binding with a K_i of 21.1 mM. Although the refined positions of both the nitrogen and the oxygen of the amide are within potential hydrogen-bonding distance to protein atoms (O to N Leu136 and OH8 Wat872 and N to OH0 Wat887), these positions are not supported by the final $2F_o - F_c$ map. It is concluded that these atoms are mobile. The waters OH4 Wat847 and OH2 Wat890 are supported by density, and these are in the position expected for the amide moiety and would be displaced by binding. The absence of a firmly located amide group and the failure to displace the waters are consistent with the poor K_i for **25**. The complex with the anilide **26** gave a surprising result. The modeling predicted and the structure confirmed that the compound made a number of favorable interactions, and yet the kinetic studies show that this is a poorer inhibitor (K_i = 3.6 mM) than **23** (K_i = 1.0 mM). The sulfur to ND2 Asn284 distance is 3.2 Å. The carbonyl oxygen is hydrogen-bonded to OH0 Wat887 and the nitrogen to OD1 Asp339. Waters OH4 Wat847 and OH2 Wat890 are displaced. The aromatic group makes a number of van der Waals interactions, including a contact 3.2 Å to NE2 His341 and 4.0 Å to N Phe285. In contrast to the aromatic derivatives of the β-amides, the thio amide places the aromatic group farther into the β-pocket, and there are no van der Waals contacts from the aromatic ring to Asp339.

A possible explanation for the less favorable K_i of **26** compared with **23** is that the favorable binding achieved by compound **23** is due to the thiolate/asparagine interaction, an interaction that is available to this compound but not to the thio-substituted compounds. Hence, despite the favorable interactions made by other groups of **26**, these do not fully compensate the loss of a thiolate interaction. The fluoro anilide **27** bound poorly and was not analyzed in detail. The hydrazide **28** did not bind at the catalytic site, but bound at the inhibitor site with the dinitrophenyl group sandwiched between the aromatic groups of Phe285 and Tyr613. The dinitrophenyl moiety appears to be the minimum requirement for binding at this site. None of the other aromatic compounds (e.g., **4–6**, **14**, **15**, and **26**) bind here.

DISCUSSION

The biological activity of the glucose analogue inhibitors has been measured by the kinetic inhibition constant, K_i, and the Hill coefficient. These parameters measure the ability of the compound to compete with substrate Glc-1-P for the catalytic site in the phosphorylase–AMP–glycogen complex and to promote the T state, respectively. Experimental evidence [discussed in Martin et al. (1991)] suggests that for glucose the inhibition constant K_i and the dissociation constant K_D are similar, and hence in comparative studies we may take differences in K_i values for closely related compounds to measure the difference in dissociation constant and, hence, the differences in the affinities of the enzyme for these compounds. This work has focused on the molecular interactions that give rise to changes in affinity and, in particular, those features that are important for the design of a tight inhibitor.

The combined X-ray crystallographic and kinetic analyzes of the glucose analogue complexes with GP*b* have shown that diversity in affinity can be achieved with small modifications. α-D-Glucose and β-D-glucose exhibit different K_i values (1.7 and 7.6 mM, respectively). The structural results show that in the α-D-glucose complex there is a hydrogen bond from the α-1-OH through a water molecule to an aspartate residue. Attempts to study the binding of β-D-glucose in GP crystals were thwarted by the rapid mutarotation of β-D-glucose to give an equilibrium mixture with composition 36% α and 64% β and by the poorer affinity of the β-D-glucose for GP (N. G. Oikonomakos, unpublished results). Model building studies show that, with the glucopyranose ring in the same position as for α-D-glucose the β-1-hydroxyl group would be placed in a mixed polar/nonpolar environment with no hydrogen bond to the protein. The α-**1** and β-**11** heptonamides show similar K_i values (0.37 and 0.4 mM, respectively), but these similar inhibition constants are achieved with different interactions by the C-amide groups at the 1-position. In the α-amide **1** there are two hydrogen bonds through water molecules to the protein, while in the β-amide **11** there is one good and one poor hydrogen bond directly to different protein atoms. Thus, a 5-fold and a 17-fold improvement in the inhibition constant are achieved compared to the parent glucose compounds by different sets of hydrogen bonds. The similarity in the inhibition constants indicates that the hydrogen bonds through water can contribute binding energies similar to those of hydrogen bonds directly from the ligand to the protein.

The improvement in the inhibition constant can easily be perturbed, as shown by the addition of a methyl group to **1** to form the α-methyl amide **2**. Compound **2** has a 100-fold larger K_i than compound **1**. The structural results show that **2** adopts a skew boat conformation, and this results in fewer hydrogen bonds from the glucosyl portion of the glucose analogue to the enzyme than were observed for analogues in the chair conformation. The skew boat conformation for the ring of **2** was the first observation of this conformation for an unsubstituted glucopyranose derivative (Watson et al., 1993). The unusual conformation is observed both in the single-crystal structure and in the complex with GP and, hence, does not appear to be a consequence of crystal lattice forces nor of binding constraints by GP.

In the present work, four other compounds were found to exhibit the skew boat conformation (compounds **3–6**), but other related compounds **7**, **8**, and **10** had normal chair conformations. This suggests that the balance between chair and skew boat is delicate and sensitive to the nature of the additional atoms attached to the α-C-amide group. In the limited number of compounds studied, it appears that the addition of nonpolar atoms to the α-C-amide group results in compounds with the skew boat conformation, while the addition of polar atoms allows retention of the chair conformation. A possible explanation for these conformational differences is suggested by the role of a water molecule observed in the GP complexes with the chair conformation. It is suggested that hydration by a water molecule that can hydrogen bond to the polar groups, as well as the amide group, may provide stabilization energy that is sufficient to favor the chair conformation. Such a mechanism for stabilization is not confined to the GP glucose analogue complex, but could also operate in solution and in the solid state.

Attempts to improve binding by additional hydrogen bonds did not always result in as large an improvement as expected. The changes in energy for the additional hydrogen bond between compounds **2** and **3**, compounds **4** and **5**, and compounds **14** and **15** are between 0.4 and 0.6 kcal/mol. Compounds **3**, **5**, and **15** contain an extra hydroxyl group compared to their partners. The difference in binding energy is less than might be expected for a hydrogen bond between a hydroxyl group and an aspartic acid residue or a hydroxyl group and a histidine. Although a direct comparison must take into account all of the other subtle shifts in atoms and changes in van der Waals contacts, this small difference in binding energy of closely related compounds can most easily be explained by desolvation effects. The energy required to remove the hydroxyl group from the bulk water and place it in the buried environment of the catalytic site of GP is only just compensated by the favorable binding energy achieved by a hydrogen bond to the protein.

Dehydration effects appear to be especially important in the rationalization of the affinities of the hydrazide compounds. The α-hydrazide **7** exhibits an 8-fold poorer inhibition constant than the α-C-amide **1**, despite similar numbers of hydrogen bonds. Likewise, comparison of the structures of GP complexed with the β-methyl amide **12** and with the corresponding hydrazide **17** shows nearly identical positions for the C1-substituent atoms, and yet **12** has a 2.5-fold better inhibition constant than **17**. In the complex with **17** the second nitrogen hydrogen bonds through water to the protein, while in the complex with **12** the methyl group makes satisfactory van der Waals interactions and the water molecule is displaced. It appears that the energy required to dehydrate the hydrazides on transfer to the catalytic site is not fully compensated by the hydrogen bonds made to the protein and that displacement of a water molecule achieved by a methyl group leads to more favorable binding energy than a hydrogen bond to this water.

The β-methyl amide **12** (K_i = 0.16 mM) is the best inhibitor of this series. The approximately 50-fold improvement in K_i over the parent β-D-glucose compound is achieved with one good hydrogen bond and favorable entropic energy changes brought about by the transfer of a methyl group from bulk solvent to the protein and displacement of a water at the catalytic site. Comparison of the structures of the complexes with the methyl amide **12** and the methyl ester **22** and the kinetic constants for these compounds allows the calculation of the strength of the hydrogen bond made in the complex with **12** of 1.7 kcal/mol. The atoms of these two complexes superimpose almost exactly, and the only difference is that in the compound **12** complex there is a hydrogen bond between the amide nitrogen and the main-chain carbonyl oxygen of His377, while in the complex with compound **22** this position is occupied by an oxygen with slight displacement of the main-chain oxygen of His377. Thus, the energy difference measures the difference between a favorable hydrogen bond and a slight repulsive van der Waals energy between two oxygen atoms 3.5 Å apart.

A salutary message from this work has been the observation that, in attempting to engineer additional favorable hydrogen bonds or van der Waals interactions, other favorable contacts are sometimes lost. The results with the α-heptonamide series show that minor modifications such as the addition of a methyl group can have substantial effects on K_i and that these effects are interpretable from the structural results (e.g., compounds **1** and **2**). The accommodation of additional groups sometimes appears to perturb favorable interactions, so that the overall binding energy of the substituted compound is less than that of the unsubstituted material. This is observed in complexes with **3** and **5**, where the need to hydrogen bond the terminal hydroxyl group in the buried environment of the enzyme leads to weakening of the hydrogen bond from O7 to N Leu136, which is observed in **4**, a compound that lacks the hydroxyl group. Likewise in the β-series, **14** and **15** do not have strong hydrogen bonds to the amide groups. In order to accommodate the phenyl group and to make favorable van der Waals contacts with this bulky group, the potential hydrogen-bond distances to the amide group have been lengthened. The series of compounds shows the difficulty in improving on the β-methyl amide. Attempts to engineer new hydrogen bonds were not as successful as might be predicted, partly because of the mixed polar/nonpolar nature of the pocket and partly because of the need to dehydrate polar groups on transfer to the protein. Attempts to accommodate other groups in the β-pocket can lead to perturbation of the favorable binding mode of the glucosyl and amide portions of the molecule.

In the complexes with the β-anilides **14** and **15**, there is a potential interaction between the carboxylate of Asp339 and the aromatic ring reminiscent of a weak aromatic/polar hydrogen bond (Burley & Petsko, 1988). In order to make this contact, the carboxylate group rotates 90° about the CB–CG bond. However, a similar flip is seen in the complex with the cyclopropyl amide **20**, and hence the change appears to be associated with the accommodation of extra groups rather than the need to hydrogen bond.

The ability of the compounds to promote the T state and, hence, lead to activation of the phosphatase against GP*a* and relieve the inhibition of the glycogen synthase activation by GP*a* is an important parallel property of these inhibitors. We note that the best inhibitor, as judged from K_i values, does not always exhibit the greatest Hill coefficient. The Hill coefficient for glucose is 1.5. The corresponding value for the α-heptonamide **1** is also 1.5, but the β-heptonamide **11** and the best inhibitor **12** have lower Hill coefficients (1.3 and 1.2, respectively), suggesting poorer T-state-stabilizing properties for the latter compounds. On the other hand, compounds **9**, **18**, and **22** show Hill coefficients of 1.7, which is significantly greater than that of glucose, and this suggests that these inhibitors may prove effective in physiological assays despite their relatively poor K_i values (between 1.6 and 2.8 mM). Compound **9** cracked the crystals, so there are no structural data available. It is not easy at this stage to rationalize why **18** and **22** should be good T-state inhibitors. Both have in common that they displace OH4 Wat847 and do not make strong hydrogen bonds with their substituent groups. OH4 Wat847 is hydrogen-bonded to Asp339 and does not play a role in the T to R transition. These properties and the ability of the inhibitors to influence the activities of phosphorylase and glycogen synthase will be addressed in future work.

It is not easy to estimate how potent the glucose analogue inhibitor of GP*a* must be in order to become a pharmaceutical agent. The studies aim to produce a compound that can modulate glycogen metabolism and not totally inhibit an enzyme as, for example, might be required for an antiviral or antibacterial agent. Witters and Avruch (1978) noted that when GP*a* activity was lowered below a certain threshold, small changes to decrease the phosphorylase activity were accompanied by large changes in glycogen synthase activity. In hepatocytes this threshold occurred in response to 30–50 mM glucose. Hence, we might require a glucose analogue inhibitor to be as effective as glucose, but at a very much lower concentration that would be acceptable for a pharmaceutical product. If we take a nominal dose of 300 mg for an average adult, then to mimic the effects on the inhibition of phosphorylase that are achieved at 50 mM glucose would

require the agent to exhibit a K_i of approximately 1 μM. The calculation assumes that all of the compound reached its target. In order to take into account absorption and bioavailability, a K_i an order of magnitude lower would probably be needed. Clearly, there is some way to go in our present inhibitor design studies to achieve a lowering of K_i by an additional 3 orders of magnitude. The current work has shown that such improvements can be achieved by small modifications that lead to only one improved hydrogen bond and displacement of a water. Further work is in progress.

ACKNOWLEDGMENT

We are grateful to Mr. S. E. Zographos for his help in the initial stages of the kinetic experiments. We are grateful to Dr. M. E. M. Noble for help with his program XOBJECTS for production of the figures.

REFERENCES

Abdel-Meguid, S. S., Zhao, B., Murthy, K. H. M., Winborne, E., Choi, J., DesJarlais, R. L., Minnich, M. D., Culp, J. S., Debouck, C., Tomaszek, T. A., Jr. Meek, T. D., & Dreyer, G. B. (1993) *Biochemistry 32*, 7972–7980.

Acharya, K. R., Stuart, D. I., Varvil, K. M., & Johnson, L. N. (1991) *Glycogen Phosphorylase b*, 1st ed., World Scientific Press, Singapore.

Alemany, S., & Cohen, P. (1986) *FEBS Lett. 198*, 194–202.

Appelt, K., Bacquet, R. J., Bartlett, C. A., Booth, C. L. J., Freer, S. T., Fuhry, M. M., Gehring, M. R., Herrmann, S. M., Howland, E. F., Janson, C. A., Jones, T. R., Kan, C., Kathardekar, V., Lewis, K. K., Marzoni, G. P., Matthews, D. A., Mohr, C., Moomaw, E. W., Morse, C. A., Oatley, S. J., Ogden, R. C., Reddy, M. R., Reich, S. H., Schoettlin, W. S., Smith, W. W., Varney, M. D., Villafranca, J. E., Ward, R. W., Webber, S., Webber, S. E., Welsh, K. M., & White, J. (1991) *J. Med. Chem. 34*, 1925–1934.

Baldwin, J. J., Smith, G., Springer, J. P., & Murcko, M. (1992) *Chem. Des. Automat. News 7*, 27–37.

Barford, D., & Johnson, L. N. (1989) *Nature 340*, 609–614.

Barford, D., Hu, S.-H., & Johnson, L. N. (1991) *J. Mol. Biol. 218*, 233–260.

Beddell, C. R., Goodford, P. J., Kneen, G., White, R. D., Wilkinson, S., & Wootton, R. (1984) *Br. J. Pharmacol. 82*, 397–407.

Bollen, M., & Stalmans, W. (1992) *Crit. Rev. Biochem. Mol. Biol. 27*, 227–281.

Brunger, A. T. (1988) *J. Mol. Biol. 203*, 803–816.

Brunger, A. T. (1989) *Acta Crystallogr., Sect. A 45*, 42–50.

Brunger, A. T., Karplus, M., & Petsko, G. A. (1989) *Acta Crystallogr., Sect. A 45*, 50–61.

Burley, S. K., & Petsko, G. A. (1988) *Adv. Protein Chem. 39*, 125.

Chapman, M. S., Minor, I., Rossmann, M. G., Diana, G. D., & Andries, K. (1991) *J. Mol. Biol. 217*, 455–463.

Cohen, P. (1992) *Trends Biochem. Sci. 17*, 408–413.

DeFronzo, R. A. (1988) *Diabetes 37*, 667–687.

Dent, P., Lavoine, A., Nakielny, S., Caudwell, F. B., Watt, P., & Cohen, P. (1990) *Nature 348*, 302–308.

Ealick, S. E., Babu, Y. S., Bugg, C. E., Erion, M. D., Guida, W. C., Montgomery, J. A., & Secrist, J. A., III (1991) *Proc. Natl. Acad. Sci. U.S.A. 88*, 11540–11544.

Engers, H. D., Shechosky, S., & Madsen, N. B. (1970) *Can. J. Biochem. 48*, 746–754.

Goekjian, P. G., Wu, T., & Kishi, Y. (1991) *J. Org. Chem. 56*, 6412–6422.

Hartmann, H., Probst, I., Jungermann, K., & Creutzfeldt, W. (1987) *Diabetes 36*, 551–555.

Hers, H. G. (1976) *Annu. Rev. Biochem. 45*, 167–189.

Howard, A. J., Gilliland, G. L., Finzel, B. C., Poulos, T. L., Ohlendorf, D. H., & Salemme, F. R. (1987) *J. Appl. Crystallogr. 20*, 383–387.

Jacobo-Molina, A., Ding, J., Nanni, R. G., Clark, A. D., Jr., Lu, X., Tantillo, C., Williams, R. L., Kamer, G., Ferris, A. L., Clark, P., Hizi, A., Hughes, S. H., & Arnold, E. (1993) *Proc. Natl. Acad. Sci. U.S.A. 90*, 6320–6324.

Johnson, L. N. (1992) *FASEB J. 6*, 2274–2282.

Johnson, L. N., Madsen, N. B., Mosely, J., & Wilson, K. S. (1974) *J. Mol. Biol. 90*, 703–717.

Johnson, L. N., Hadju, J., Acharya, K. R., Stuart, D. I., McLauchlin, P. J., Oikonomakos, N. G., & Barford, D. (1989) Glycogen Phosphorylase b. in *Allosteric Enzymes* (Herve, G., Ed.) p 81, CRC Press, Boca Raton, FL.

Jones, T. A. (1978) *J. Appl. Crystallogr. 11*, 268–272.

Jones, T. A. (1985) *Methods Enzymol. 115*, 157–171.

Kabsch, W. (1988a) *J. Appl. Crystallogr. 21*, 67–71.

Kabsch, W. (1988b) *J. Appl. Crystallogr. 21*, 916–924.

Kim, K. H., Willingmann, P., Gong, Z. X., Kremer, M. J., Chapman, M. S., Minor, I., Oliveira, M. A., Rossmann, M. G., Andries, K., Diana, G. D., Dutko, F. J., McKinlay, M. A., & Pevear, D. C. (1993) *J. Mol. Biol. 230*, 206–227.

Kohlstaedt, L. A., Wang, J., Friedman, J. M., Rice, P. A., & Steitz, T. A. (1992) *Science 256*, 1783–1790.

Leatherbarrow, R. J. (1987) *Enzfitter, A Non-Linear Regression Data Analysis Program for the IBM-PC*, Elsevier Biosoft, Cambridge, U.K.

Lemieux, R. U., & Koto, S. (1974) *Tetrahedron 30*, 1933–1944.

Madsen, N. B., Kasvinsky, P. J., & Fletterick, R. J. (1978) *J. Biol. Chem. 253*, 9097–9101.

Madsen, N. B., Shechosky, S., & Fletterick, R. J. (1983) *Biochemistry 22*, 4460–4465.

Martin, J. L., Johnson, L. N., & Withers, S. G. (1990) *Biochemistry 29*, 10745-10757.

Martin, J. L., Veluraja, K., Ross, K., Johnson, L. N., Fleet, G. W. J., Ramsden, N. G., Bruce, I., Orchard, M. G., Oikonomakos, N. G., Papageorgiou, A. C., Leonidas, D. D., & Tsitoura, H. S. (1991) *Biochemistry 30*, 10101–10116.

Newgard, C. B., Nakano, K., Hwang, P. K., & Fletterick, R. J. (1986) *Proc. Natl. Acad. Sci. U.S.A. 83*, 8132–8136.

Newgard, C. B., Hwang, P. K., & Fletterick, R. J. (1989) *Crit. Rev. Biochem. Mol. Biol. 24*, 66–99.

Oikonomakos, N. G., Melpidou, A. E., & Johnson, L. N. (1985) *Biochim. Biophys. Acta 832*, 248–256.

Quiocho, F. A. (1989) *Pure Appl. Chem. 61*, 1293–1306.

Shoichet, B. K., Stroud, R. M., Santi, D. V., Kuntz, I. D., & Perry, K. M. (1993) *Science 259*, 1445–1450.

Sprang, S. R., Fletterick, R. J., Stern, M. J., Yang, D., Madsen, N. B., & Sturtevant, J. S. (1982a) *Biochemistry 21*, 2036–2048.

Sprang, S. R., Goldsmith, E. J., Fletterick, R. J., Withers, S. G., & Madsen, N. B. (1982b) *Biochemistry 21*, 5364–5371.

Stalmans, W., De Wulf, H., Hue, L., & Hers, H. G. (1974) *Eur. J. Biochem. 41*, 127–134.

Tripos Associates Inc. (November, 1992) Sybyl Molecular Modeling Software, St. Louis, MO.

von Itzstein, M., Wu, W., Kok, G. B., Pegg, M. S., Dyason, J. C., Jin, B., Phan, T. V., Smythe, M. L., White, H. F., Oliver, S. W., Colman, P. M., Varghese, J. N., Ryan, D. M., Woods, J. M., Bethell, R. C., Hotham, V. J., Cameron, J. M., & Penn, C. R. (1993) *Nature 363*, 418–423.

Watson, K. A., Mitchell, E. P., Johnson, L. N., Son, J. C., Bichard, C. J. F., Fleet, G. W. J., Ford, P., Watkin, D. J., & Oikonomakos, N. G. (1993) *J. Chem Soc., Chem Commun. 7*, 654–656.

Witters, L. A., & Avruch, J. (1978) *Biochemistry 17*, 406–410.